*J. Fluid Mech.* (1978), *vol.* 86, *part* 4, *pp.* 623–639
*Printed in Great Britain*



# Non-Newtonian flow characteristics in a steady two-dimensional flow

By THOMAS B. GATSKI

Department of Aerospace Engineering, The Pennsylvania State University, University Park, Pennsylvania 16802†

AND JOHN L. LUMLEY

Sibley School of Mechanical and Aerospace Engineering, Cornell University, Ithaca, New York 14853

(Received 21 January 1977 and in revised form 21 October 1977)

The two-dimensional steady flow of a non-Newtonian fluid (a dilute polymer solution) is examined. The flow domain is composed of a parallel-walled inflow region, a contraction region in which the walls are rectangular hyperbolae, and a parallel-walled outflow region. The problem is formulated in terms of the vorticity, stream function and appropriate rheological equation of state, i.e. an Oldroyd-type constitutive equation (with no shear-thinning) for the total shear and normal-stress components. Computational results from the numerical solution of the equations are presented. In particular, the molecular extension and pressure distribution along the centre-line are presented as well as contour plots of the different flow variables. The alignment of the molecules with the principal axes of strain rate is shown by a qualitative comparison of the streamwise normal-stress contours with contours of the eigenvalues of the strain-rate matrix.

## 1. Introduction

An understanding of the flow of dilute suspensions of long-chain macromolecules requires information about such basic flow variables as velocity and pressure and, in addition, information about stress and strain-rate fields. Such media display the drag-reduction phenomenon in turbulent liquid flow and, of course, are relevant in polymer processing (although here the concentration may be higher, the similarity of the constitutive equations produces similar local behaviour). Our motivation arises from the observation of extensive drag reduction caused by the addition of long-chain linear macromolecules to a turbulent flow, the Toms phenomenon (Toms 1948). It has been suggested (e.g. Lumley 1969; Peterlin 1970) that the relevant mechanism in the drag-reducing process is the extension of the molecules in a fluctuating strain-rate field of a turbulent flow. Such a molecular extension causes an increase in tensile viscosity, and hence in effective viscosity, which damps out the small eddies. This then lessens the Reynolds stress in the turbulent buffer layer and shifts to a point further from the wall the reduction of the mean profile slope. It should be noted that no significant molecular extension occurs in the viscous sublayer since the molecules are

† Permanent address: NASA Research Center, Hampton, Virginia 23665.

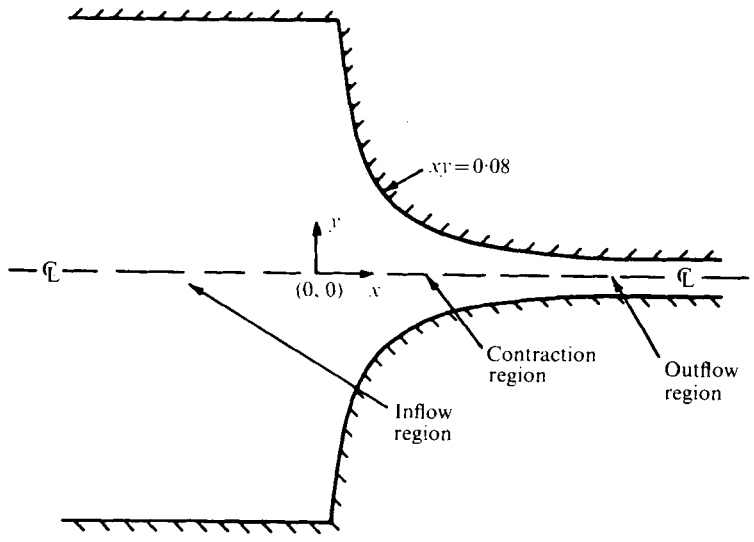


FIGURE 1. Flow domain.

not aligned long enough with the principal axes of the mean strain-rate field owing to the strength of the mean vorticity field. We shall not address here the problem of turbulent flow of a non-Newtonian fluid, although there are closure assumptions for the turbulent problem that make it at least numerically tractable. (Higher-order closures such as stress-equation models, however, make even the Newtonian problem burdensome.) Rather, it appears advantageous first to consider a laminar problem with a suitable constitutive equation for the behaviour of this viscoelastic fluid and to solve a coupled set of partial differential equations governing the motion of the fluid. In light of the above areas of application and, in particular, for molecular extension it is desirable to study an extensional flow field (Huilgol 1975) to understand better the dynamics of such extensions. In polymer-processing applications understanding the basic flow structure as well as stress and strain-rate fields in converging flows in general is of much importance. Such a combination of flow fields can be obtained in the geometry shown in figure 1; here a two-dimensional contraction region whose boundaries are rectangular hyperbolae (thus making the flow along the centre-line an extensional flow) is preceded and followed by parallel-walled inflow and outflow regions (these parallel-walled regions aid in setting up the computational problem). Recently Black & Denn (1975) have applied a perturbation technique (expansion in the Weissenberg number) to the solution of sink flow of a viscoelastic fluid. Their analytical results were then compared with numerical results (Black, Denn & Hsaio 1975) obtained for a bounded converging flow with a 90° corner and were also compared with numerical results for a geometry similar to figure 1 but with the contraction region bounded by linear line segments. Here we are taking the analysis further in that we are numerically solving the motion (specifically, our formulation is in terms of the vorticity and stream function) and stress-field equations simultaneously, for the time-independent case. Our numerical technique is the finite-difference method, and is used to solve equations for the vorticity, stream function, shear and normal-stress components and strain-rate tensor throughout the region of figure 1. The

constitutive equation here is a three-constant Oldroyd model for the total stress tensor (the general form is that of the Oldroyd *B* fluid, Oldroyd 1950) which corresponds to a convective Maxwell model for the extra stress due to the presence of the molecules. It is based on the assumption of a linear spring constant, a constant friction factor and no submolecules, i.e. the molecule is modelled by a simple spring connecting two dumb-bells. Although not used here, Tanner (1975*a*) has proposed a model which accounts for nonlinear springs, using an approximation to the inverse Langevin function, and for a variable friction factor, based on the square root of the number of submolecules. His results, although based on numerical computations, did not involve solving the stress equations in conjunction with an appropriate motion (or vorticity) equation but simply involved specifying the velocity field and obtaining results from the stress equations. Duda & Vrentas (1973) have obtained time-dependent numerical solutions (finite-difference technique) of the equations describing the non-Newtonian flow from a pipe of infinite length, through a sudden contraction to an infinitely long, smaller tube. The fluid considered in their work was a nonlinear viscous fluid, i.e. a Powell–Eyring fluid, and the investigation centred on entrance-flow effects on the size of the developed recirculation region. Numerical modelling of non-Newtonian flows has also been done by Townsend (1973). He applied the finite-difference technique to the Oldroyd equation for unsteady flow in a straight pipe of circular cross-section, but here, owing to the flow geometry, the nonlinear advection terms did not appear in the governing equations.

Let us now turn to establishing the appropriate governing differential equations used in this investigation; for the interested reader the numerical procedure used can be found in Gatski (1978).

## 2. Governing equations and boundary conditions

We are considering here a two-dimensional laminar flow of a non-Newtonian viscoelastic fluid; the problem can be formulated in terms of the vorticity and stream function and, of course, an appropriate constitutive equation. Since the fluid is incompressible (the motion then being isochoric and the velocity vector solenoidal) and there are no external body forces, the time-independent (dimensionless) vorticity equation is

$$u_j \omega^l_{,j} = \epsilon^{lni} g_{ik} \tau^{kj}_{,jm}, \tag{2.1}$$

where

$$\omega^l = \epsilon^{lni} u_{i,n}. \tag{2.2}$$

In general in this paper, subscripts and superscripts preceded by a comma indicate covariant and contravariant spatial differentiation, respectively. As for the constitutive equation, Giesekus (1966) has shown that a dilute solution of linear-spring dumb-bells can be described by a convective Maxwell model for the additional stress due to the presence of the molecules. Thus for the total stress tensor, i.e. the part contributed by the polymer as well as the usual Newtonian linear relationship with the strain rate, the appropriate (dimensionless) constitutive equation is

$$\tau^{kj} + \lambda_1 \frac{\delta \tau^{kj}}{\delta t} = \frac{2(1 + c[\eta])}{R_s} S^{kj} + \frac{2\lambda_1}{R_s} \frac{\delta S^{kj}}{\delta t}, \tag{2.3}$$

where

$$\delta \tau^{kj}/\delta t = u^m \tau^{kj}_{,m} - u^k_{,m} \tau^{mj} - u^j_{,m} \tau^{km}, \tag{2.4}$$

$$S^{kj} = \tfrac{1}{2}(u^{k,j} + u^{j,k}), \tag{2.5}$$

$R_s$ is the solvent Reynolds number based on the mean inflow velocity $U$ at the entrance to the flow domain, $g^{jk}$ is the contravariant metric tensor, $\lambda_1$ is a time constant related to the molecular relaxation time, $c$ is the concentration (in parts per million by weight) and $[\eta]$ is the intrinsic viscosity (Peterlin 1966). It should be noted that the concentration $c$ can be related to the number of molecules per unit volume through Avogadro's number and the molecular weight of the polymer, and in the limit of zero concentration $\nu c[\eta]$, where $\nu$ is the kinematic viscosity, is simply the polymer-contributed shearing viscosity (Lumley 1971; cf. Tanner & Stehrenberger 1971). Also note that the non-dimensionalization has introduced the solvent Reynolds number $R_s$ into the constitutive equation (for the results presented here $R_s = 5000$), and that in the limit of zero concentration the usual Newtonian relationship is recovered. Equation (2.4) can be recognized as the Oldroyd convective derivative (Oldroyd 1950) and the constitutive equation (2.3) corresponds to the one for the Oldroyd $B$ fluid (the $B$ fluid exhibits the positive Weissenberg effect; Oldroyd 1950). This model does not exhibit any shear-thinning behaviour, i.e. variation of the apparent viscosity with shear. The generality used in writing the above vorticity and constitutive equations was necessary because of the irregular boundary and the need to specify the boundary conditions on the different tensor quantities in a co-ordinate system other than a Cartesian one. Before considering the boundary conditions, let us first rewrite the vorticity and constitutive equations in the more familiar Cartesian frame; with the velocity given by

$$\mathbf{u} = (u(x,y), v(x,y), 0) \tag{2.6}$$

these equations become

$$u\omega_x + v\omega_y = \partial(\psi,\omega)/\partial(x,y) = \tau^{12}_{xx} - \tau^{12}_{yy} + (\tau^{22} - \tau^{11})_{xy}, \tag{2.7}$$

$$\tau^{12} + \lambda_1[u\tau^{12}_x + v\tau^{12}_y - \tau^{22}u_y - \tau^{11}v_x] = \frac{2(1+c[\eta])}{R_s} S^{12} + \frac{2\lambda_1}{R_s}[uS^{12}_x + vS^{12}_y - S^{22}u_y - S^{11}v_x], \tag{2.8}$$

$$\tau^{11} + \lambda_1[u\tau^{11}_x + v\tau^{11}_y - 2\tau^{12}u_y - 2u_x\tau^{11}] = \frac{2(1+c[\eta])}{R_s} S^{11} + \frac{2\lambda_1}{R_s}[uS^{11}_x + vS^{11}_y - 2S^{12}u_y - 2S^{11}u_x], \tag{2.9}$$

$$\tau^{22} + \lambda_1[u\tau^{22}_x + v\tau^{22}_y - 2\tau^{12}v_x - 2\tau^{22}v_y] = \frac{2(1+c[\eta])}{R_s} S^{22} + \frac{2\lambda_1}{R_s}[uS^{22}_x + vS^{22}_y - 2S^{12}v_x - 2S^{22}v_y], \tag{2.10}$$

$$\omega = v_x - u_y = -\nabla^2\psi, \tag{2.11}$$

where $\psi$ is the stream function. Turning our attention now to the boundary conditions let us first consider the stream function. In (2.11) it is necessary to specify either the value of $\psi$ (Dirichlet condition) or its normal derivative (Neumann condition) along the boundaries of the flow domain. Here we are doing the Dirichlet problem and begin by specifying the stream-function values at the entrance to the flow domain. It is assumed here that the inflow velocity profile is parabolic; then the stream-function values can be simply obtained by integrating the distribution from $y = 0$ (centre-line) to $y = 1{\cdot}0$ (wall). Owing to the symmetry of the flow domain the stream-function value along the centre-line must be constant ($\psi = 0$) and owing to the solid boundary the stream-function value along the parallel and curved sections must also be constant

($\psi = 1{\cdot}0$). Finally, the straight outflow section is assumed to be sufficiently long that the velocity is simply a function of $y$ (in the numerical computations on this set of equations (Gatski 1978) this assumption was found to be quite satisfactory). Now consider the vorticity equation.

From the equations it is seen that both the vorticity and the stresses need to be specified along the boundaries of the domain. Let us first determine the vorticity conditions. Along the centre-line the vorticity must be zero and at the entrance the vorticity is simply determined by differentiating the parabolic velocity profile. Along the parallel-walled sections of the solid boundary and at the exit of the domain the vorticity is given by (2.11) subject to the conditions of non-porous walls and a non-evolving flow in the streamwise direction, respectively. Since vorticity is a pseudo-vector and the only vorticity component is perpendicular to the $x, y$ plane (see figure 1), the distribution of vorticity values along the curved boundary can be determined from (2.11) or from a corresponding equation formulated in terms of a co-ordinate parallel and perpendicular to the curved boundary. Now that the boundary conditions for the kinematic variables have been specified we turn our attention to the non-Newtonian aspects of the problem, i.e. the specification of the stress boundary conditions.

Since the flow is symmetric about the centre-line, the $\tau^{12}$ shear stress is simply equal to the extra stress due to the presence of the molecules there, and, if the molecules are unstretched at the entrance, the shear stress along the centre-line is zero. As for the normal stresses, a cursory treatment of (2.9) and (2.10) reveals that these equations yield differential boundary conditions for both normal stresses along the centre-line and that the stresses are non-zero and not equal to the usual Newtonian values. At the entrance to the flow domain, the flow is assumed parallel; therefore the stress conditions applicable at the entrance are

$$\tau^{12} = 2(1 + c[\eta])\, R_s^{-1} S^{12}, \tag{2.12}$$

$$\tau^{11} = 8 R_s^{-1} \lambda_1 c[\eta]\, (S^{12})^2, \tag{2.13}$$

$$\tau^{22} = 0. \tag{2.14}$$

Note that the shear and cross-stream normal stresses are essentially Newtonian values and only the streamwise normal stress is different. In addition, note that these stress conditions are applicable for any parallel flow. Let us now consider the boundary conditions along the solid walls. Using the conditions that the tangential and normal velocities are zero along the solid boundaries, one can obtain from (2.8)–(2.10) the conditions along the parallel-walled boundaries. The shear- and normal-stress distributions that result are the same as those obtained at the entrance, i.e. (2.12)–(2.14). Along the curved section of the boundaries the tangential and normal velocities are, of course, zero; however, even though the above relationships between stress and the strain rate still hold, one must now refer to physical components of the stress and strain-rate tensors in a co-ordinate system parallel and perpendicular to the boundaries. This means that in solving the governing equations, which are expressed in terms of Cartesian components, one needs to transform the physical components of the second-order tensor quantities in the curvilinear system to the respective Cartesian components (Gatski 1978). Finally, the only stress conditions that need to be specified are those at the exit of the flow domain. These conditions can be easily determined if one

recalls that at the exit of the domain the flow was assumed parallel; hence the same assumption here allows us to use the stress conditions (2.12)–(2.14) for the exit boundary conditions. Recall at this point that the boundary conditions on the strain rate are obtainable directly from the stream function and stress distribution already presented by applying the Newtonian limit of zero molecular relaxation time and zero concentration and using the fact that the Newtonian stresses and strain rates are linearly related by $2R_s^{-1}$.

It should be noted that these boundary conditions on the various flow variables dictate the behaviour of the fluid in the interior of the domain. For example, the boundary conditions on the stresses clearly indicate that it is the streamwise normal stress that most strongly dictates the extent that the non-Newtonian fluid deviates from the behaviour of the Newtonian fluid and, as will be seen in the next section, it is this $\tau^{11}$ normal stress that is related to molecular expansion.

## 3. Molecular extension and pressure distribution

A measure of molecular extension along the centre-line can be given by the variance tensor of position $I^{ik}$ (e.g. Lumley 1971; Giesekus 1962), which for the dumb-bell model (two masses held together by an elastic restoring force) of a molecule represents the mean-square location of one mass relative to the centre of mass. The position tensor $I^{ik}$ can be related to the additional stress due to the presence of the molecules, i.e.

$$\tau^{(m)\,ik} = \left(\frac{3I^{ik}}{r^2} - \delta^{ik}\right)\frac{c[\eta]}{R_s\lambda_1}, \tag{3.1}$$

where $r$ is the equilibrium radius of the molecule and $\tau^{(m)\,ik} = \tau^{ik} - 2R_s^{-1}S^{ik}$ is the extra stress due to the presence of the molecules. By introducing the total stress tensor into (3.1), one can solve for the square root of the position tensor to obtain a measure of molecular distortion:

$$\left(\frac{3I^{ik}}{r^2}\right)^{\frac{1}{2}} = \left[\left(\tau^{ik} - \frac{2}{R_s}S^{ik}\right)\frac{R_s\lambda_1}{c[\eta]} + \delta^{ik}\right]^{\frac{1}{2}}. \tag{3.2}$$

Along the centre-line we are interested in a measure of axial extension; hence the component of interest is $I^{11}$ and (3.2) becomes

$$\left(\frac{3I^{11}}{r^2}\right)^{\frac{1}{2}} = \left[\left(\tau^{11} - \frac{2}{R_s}S^{11}\right)\frac{R_s\lambda_1}{c[\eta]} + 1{\cdot}0\right]^{\frac{1}{2}}. \tag{3.3}$$

Since the streamwise normal-stress and strain-rate distribution can be determined from the numerical solution of the motion and constitutive equations (Gatski 1978), (3.3) enables one to determine the amount of axial stretching. In order to get a theoretical estimate of the same quantity, consider the following differential equation for the tensor of molecular distribution $I^{ik}$ (e.g. Lumley 1972*a*):

$$I^{im}u_{k,m} + I^{mk}u_{i,m} - \frac{I^{ik}}{\lambda_1} = -\frac{\delta^{ik}r^2}{3\lambda_1}. \tag{3.4}$$

From this equation we can once again solve for the normalized streamwise component of the distribution tensor:

$$(3I^{11}/r^2)^{\frac{1}{2}} = (1 - 2S\lambda_1)^{-\frac{1}{2}}, \tag{3.5}$$

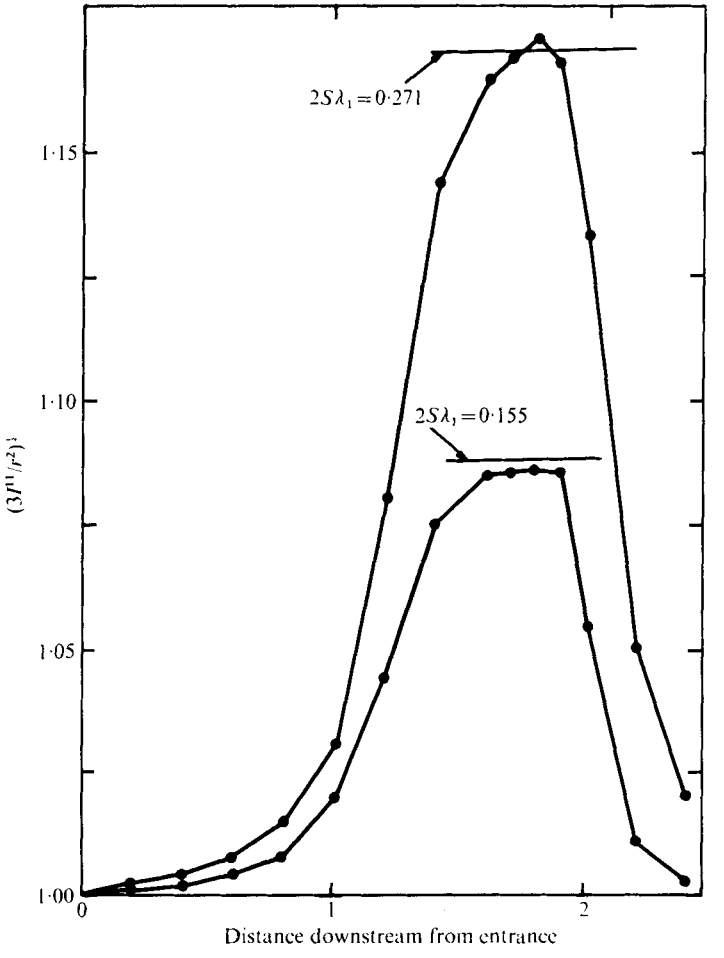


FIGURE 2. Molecular extension along centre-line of contraction.

where $S = u_x$. Note that the above expression is independent of $c[\eta]$, indicating that the only relevant parameter of the polymer additive in the flow of a dilute suspension is the molecular relaxation time $\lambda_1$. In addition note that this equation has a singularity at $2S\lambda_1 = 1$; this, of course, is physically unrealistic and is due to the fact that the motion and flow were assumed steady and, in addition, reflects an inadequacy of this linear spring model. We shall not attempt here to introduce a limit to the extension such as an upper bound corresponding to the total molecular length (e.g. Tanner 1975*b*). In figure 2 molecular extension, both theoretical and computational, is plotted *vs.* distance downstream along the centre-line for two values of $2S\lambda_1$. The values of the Reynolds number $R_s$ and $c[\eta]$ were 5000 and 1·0 respectively. These values allowed for a well-defined flow pattern and a discernible difference between the stress levels of the non-Newtonian and base Newtonian (solvent) flows. The larger value of $2S\lambda_1$ presented corresponds to a value of $\lambda_1$ of $9{\cdot}0 \times 10^{-3}$, which was the maximum value of $\lambda_1$ used owing to numerical instabilities encountered in the computations (Gatski 1978). As can be seen from the figure the molecular extension obtained from the computational data using (3.3) agrees very well with that predicted

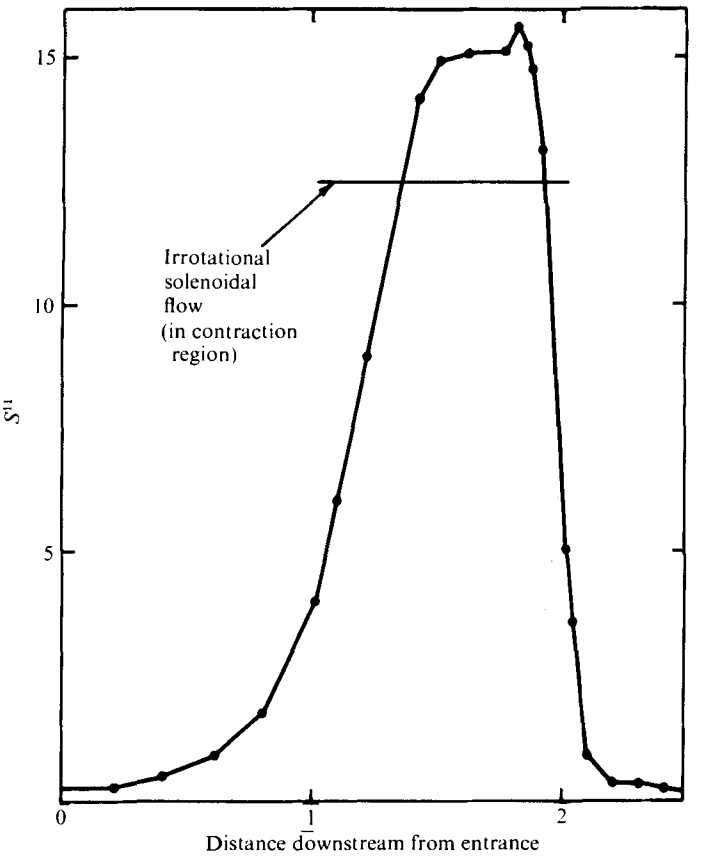


FIGURE 3. $S^{11}$ strain-rate distribution along centre-line of flow domain.

by (3.5). Notice, though, that at $2S\lambda_1 = 0{\cdot}271$ the curve has developed a small amplitude spike in the region of maximum extension. The same type of spike is found in the strain-rate distribution along the centre-line (figure 3) and is an artifact of the abrupt change in curvature at the interface between the boundaries of the contraction and outflow region in the discretized computational field. Therefore, with an increase in the relaxation time, this irregularity in the strain-rate distribution is more effectively communicated to the $\tau^{11}$ normal stress through the corresponding constitutive equation. Also included in figure 3, for comparison, is the inviscid strain-rate distribution for this particular contraction (note that $S^{11}$ scales with the contraction ratio in the inviscid problem). The magnitude of $S^{11}$ is larger in the non-Newtonian problem (and, of course, in the base Newtonian problem) because the boundary layers effectively reduce the contraction width, thus causing higher velocities and hence a larger acceleration. The region of constant strain rate is smaller because of the large recirculating flow which exists in the corner of the upper contraction region. Finally, it is of interest to look at the overall root-mean-square radius $(3I^{ii}/2r^2)^{\frac{1}{2}}$. From figure 4, it is seen that the total size of the molecular chain does increase, by virtue of the fact that the axial extension is greater than the transverse compression of the molecule. As will be seen below, this increase in size is partly a consequence of the pressure distribution on the molecule.

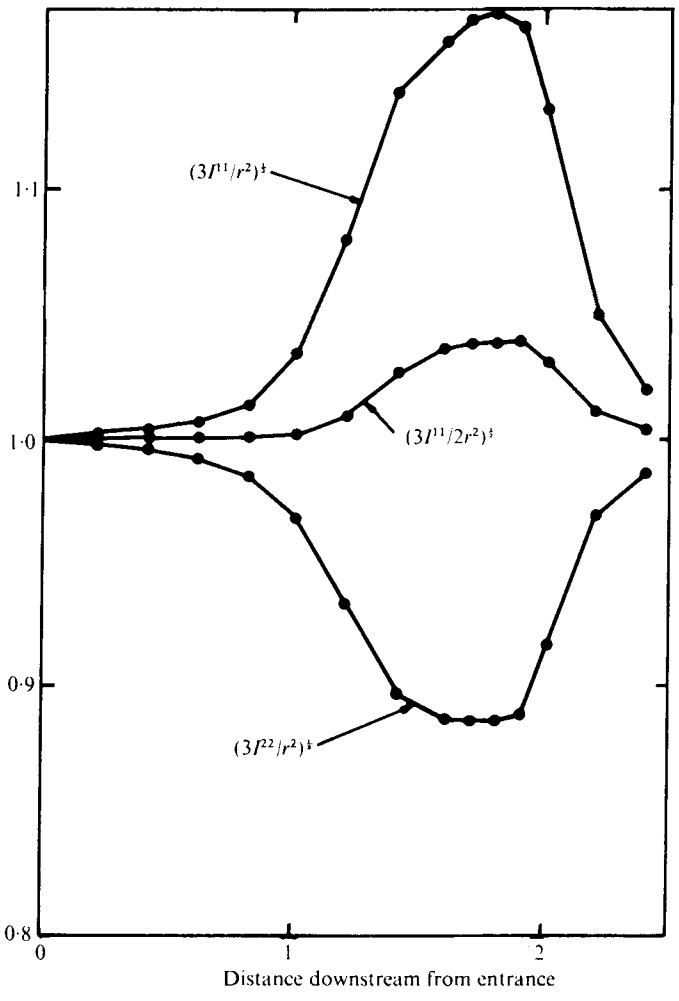


FIGURE 4. Variation of molecular distribution tensor along centre-line.

From the above, an additional result, which is of interest along the centre-line, is the pressure. It has been shown that the pressure drop decreases relative to the Newtonian value along the centre-line, i.e. for uniform axial acceleration (as was the case along the centre-line) a smaller pressure gradient is needed to maintain the non-Newtonian flow (Lumley 1972*b*; Metzner, Uebler & Chun Man Fong 1969). Figure 5 shows the Newtonian and non-Newtonian ($\lambda_1 = 9{\cdot}00 \times 10^{-3}$, $c[\eta] = 1{\cdot}0$, $R_s = 5000$) pressure distributions. As can be seen, the curves are relatively close throughout most of the contraction and begin to diverge only in the region where molecular stretching becomes dominant. In order to explain a decrease in pressure drop the effect of the transverse forces must be examined, since in the absence of these forces increasing the axial tension to produce stretching would cause an increase in the pressure drop. The pressure is the (negative) average of the normal stresses, so a decrease in the pressure drop (pressure increase) means an increase in the (negative) average normal stress. Since the axial normal stress increases (causing extensions, figures 2 and 4), or the (negative) axial normal stress decreases, the (negative) transverse normal stress must

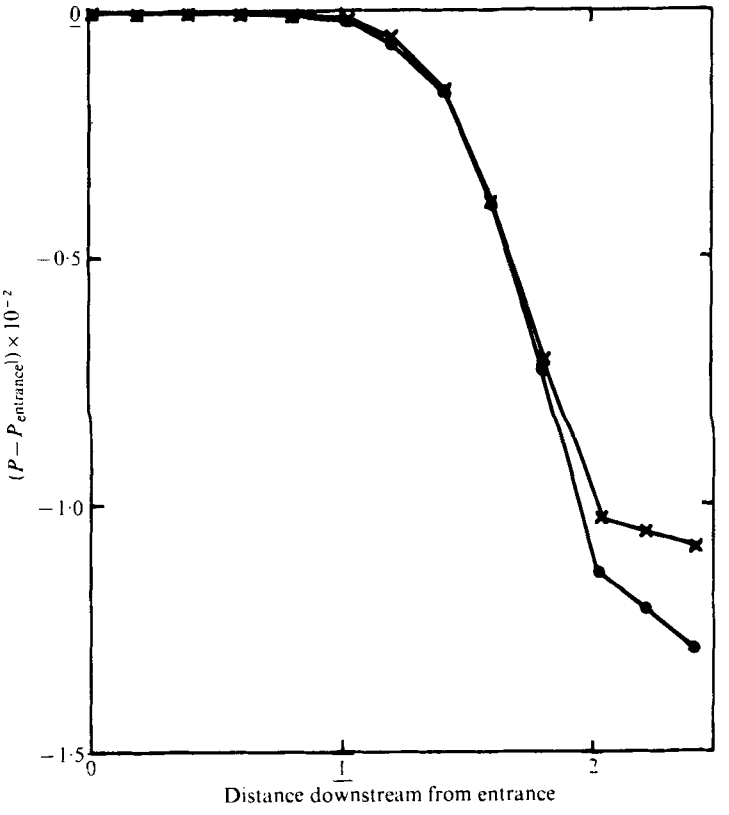


FIGURE 5. Comparison of Newtonian and non-Newtonian pressure distributions. ●, Newtonian; ×, non-Newtonian.

increase even more, resulting in an increase of the average. Thus the compressive stress required to compress the molecules transversely is greater than the tension required to stretch them axially (Lumley 1972*b*).

## 4. Contours of flow variables throughout domain

Let us now turn our attention to the contour plots of the various flow variables for the non-Newtonian flow characterized by the flow parameters $R_s = 5000$, $\lambda_1 = 9{\cdot}0 \times 10^{-3}$ and $c[\eta] = 1{\cdot}0$. As indicated earlier, details of the numerical modelling and the choice of flow parameters can be found in Gatski (1976). First, the streamlines are presented in figure 6(*a*).

As can be seen, a large recirculation region has formed in the corner of the domain. The interesting feature of this region is the fact that its size has decreased relative to that in the flow of the Newtonian fluid through the same configuration (cf. figure 6*b*); specifically, in the non-Newtonian case the separation point occurred at $x = 0{\cdot}68$ whereas in the Newtonian case it is at $x = 0{\cdot}60$. This relocation of the separation point further downstream means that in the non-Newtonian flow the fluid velocity did not decelerate as quickly as in the Newtonian case. One possible reason for this slower deceleration is that the adverse pressure gradient in the non-Newtonian flow is less

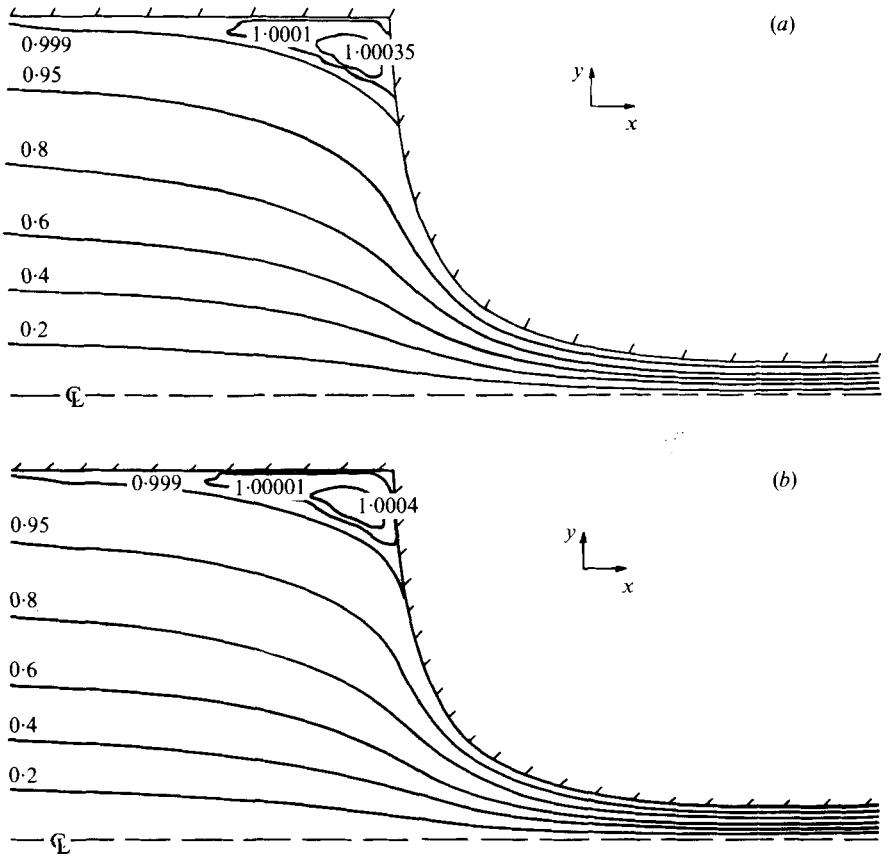


FIGURE 6. Streamlines for (*a*) a non-Newtonian and (*b*) a Newtonian fluid in the flow domain.

than that in the Newtonian case. However, figure 7 shows that this is not the case; in fact, the non-Newtonian pressure distribution near the wall ($y = 0{\cdot}98$) is higher. It would appear then that molecular stretching occurs in this region (although on a very limited scale compared with the centre-line), since molecular compression would cause a pressure decrease (relative to the Newtonian value), and that it is not a change in pressure distribution that causes the delayed separation. Further numerical tests indicated that this delay in separation was a function of concentration, i.e. a higher concentration produced further downstream separation. This increase in the term $c[\eta]$ lowers the apparent Reynolds number of the flow (recall the factor $2(1+c[\eta])\,R_s^{-1}$ in the constitutive equation) and, in addition, decreases the ratio $(1+c[\eta])^{-1}$ of the retardation time to the relaxation time (the retardation time is the time it takes for the strain to fall to $e^{-1}$ of its original value and is given here by $\lambda_1(1+c[\eta])^{-1}$). It has been found that this decrease in retardation time increases the elasticity of the fluid, causing velocity overshoots in certain time-dependent flows (Waters & King 1971). For example, in unsteady Poiseuille flow, the velocity near the wall is larger than the corresponding Newtonian velocity in the initial stages of development. An analogy with this behaviour can be formed in this steady-state problem by viewing the flow from a Lagrangian frame. Then the observed increased flow velocity can be explained by the increased elasticity effects as $c[\eta]$ is increased. Of course, since the flow is steady

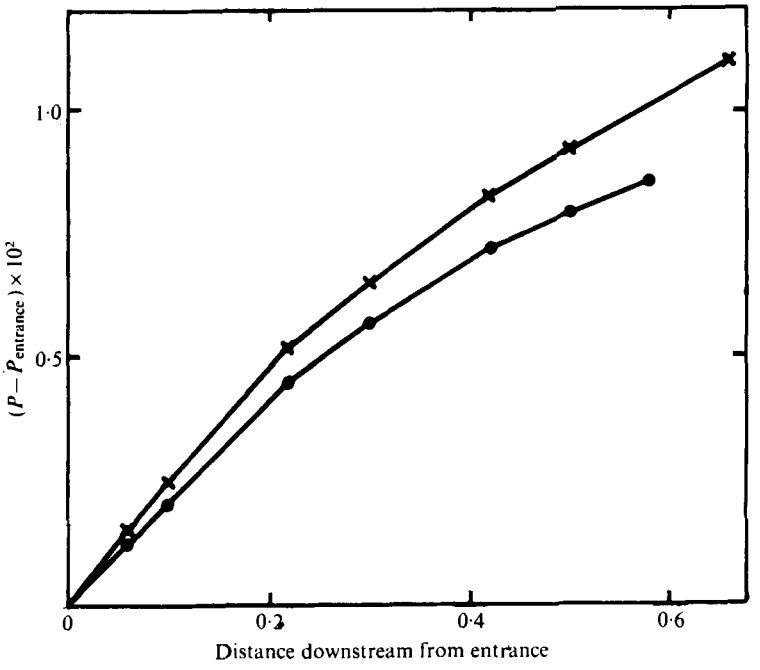


FIGURE 7. Pressure distribution near solid wall. ●, Newtonian; ×, non-Newtonian.

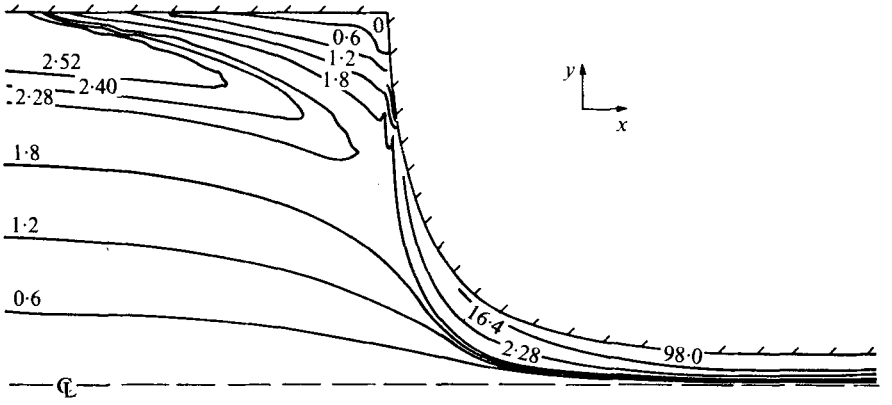


FIGURE 8. Vorticity contour lines for a non-Newtonian fluid in the flow domain.

the streamlines represent the paths (streaklines) that tracer elements would follow if injected into the flow. It should be noted that experimental results such as those obtained by Metzner *et al.* (1969) for flow from a large duct into a small tube indicate the occurrence of a larger recirculation region in the non-Newtonian flow though there was no such occurrence for the Newtonian flow in the same geometry. Here the Newtonian flow did produce a recirculation region and the geometry in this case displays a much smoother transition to the smaller outflow region. These two differences, especially the different geometry, explain the differing flow responses to the non-Newtonian fluids. Now let us briefly look at the other kinematic variable of interest, the vorticity.

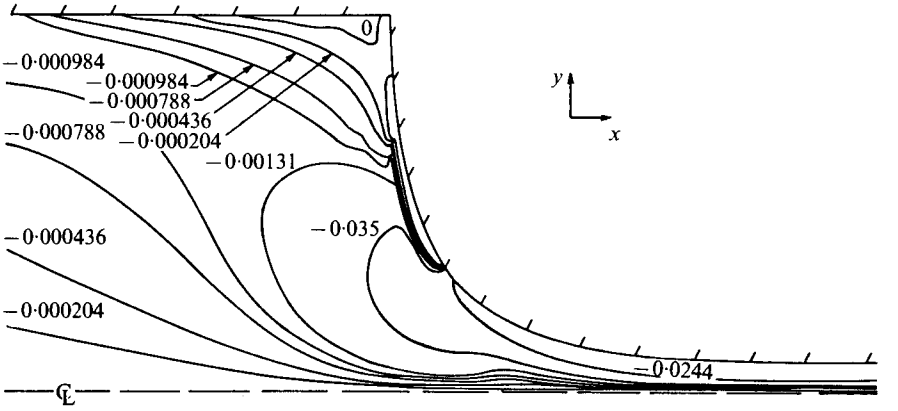


FIGURE 9. Shear-stress contour lines for a non-Newtonian fluid in the flow domain.

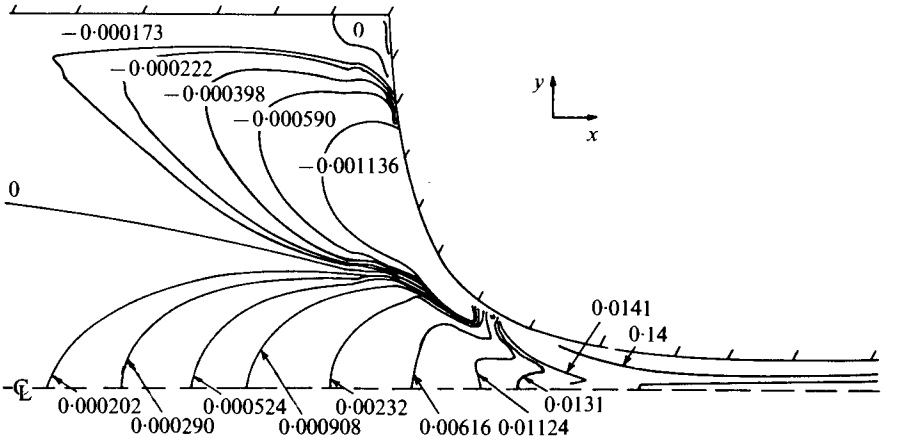


FIGURE 10. $\tau^{22}$ normal-stress contour lines for a non-Newtonian fluid in the flow domain.

Vorticity contours are shown in figure 8. Notice that the contour $\omega = 0$ along the solid boundary emanates from the points of separation and reattachment as indicated in figure 6 (*a*). This is consistent with the fact that along the solid boundary in the inflow region $\omega = u_y|_{\text{wall}}$ and this point of separation corresponds to the point of zero shear. Further examination of figure 8 reveals that large amounts of vorticity are concentrated near the contraction wall. From the stream-function data one can estimate the displacement thickness in an area midway through the contraction region (Gatski 1976). Such a calculation yields a displacement thickness of $\delta^* \sim 0{\cdot}02$. However, this result, obtained by taking the area under the velocity profile at a point in the contraction region, does not correspond to an estimate obtained using the relation $\delta^* \sim (R_s S^{11})^{-\frac{1}{2}}$, where $S^{11}$ is the strain rate at the point in question. Since here $R_s = 5000$ and $S^{11} = 15{\cdot}0$ at this point (Gatski 1976) a value of $\delta^* \sim 0{\cdot}00365$ is obtained. This discrepancy can be explained by taking into account numerical viscosity (Roache 1972, p. 64). As is well known, these numerical errors occur when one-sided or upstream differencing is used on the advection terms. This additional viscous effect is of the order of $\frac{1}{2}v\Delta$, where $\Delta$ is the grid spacing ($= 2{\cdot}0 \times 10^{-2}$) and $v$ is

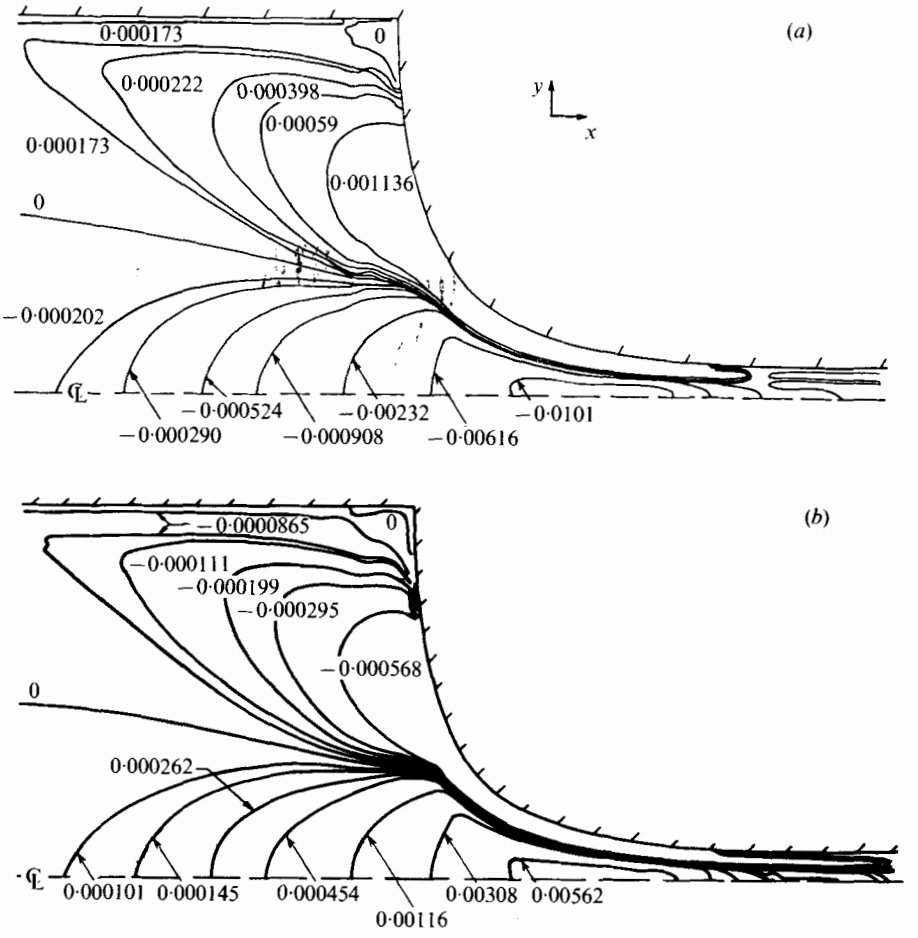


FIGURE 11. $\tau^{11}$ normal-stress contour lines for (*a*) a non-Newtonian and (*b*) a Newtonian fluid in the flow domain.

some local velocity. Near the wall $v \simeq 3{\cdot}0$ (Gatski 1976) and the artificial viscosity is $3{\cdot}0 \times 10^{-2}$ (which corresponds to a computational Reynolds number of $R_c = 33{\cdot}0$). Now letting $\delta^* \sim (v\Delta/2S^{11})^{\frac{1}{2}}$ one obtains for $\delta^*$ a new estimate of 0·0447, which is more in line with the computational result. Although artificial-viscosity errors are present the results along the centre-line, away from the wall region, should not be affected. Up to this point we have looked at the kinematic variables, the stream function and vorticity, but now let us examine the stresses, which characterize the non-Newtonian features of the flow.

First let us look at the $\tau^{12}$ shear-stress contours (figure 9) and the $\tau^{22}$ normal-stress contours (figure 10). Recall that the boundary conditions for these variables were essentially Newtonian conditions. For example, the boundary condition for the $\tau^{12}$ shear stress was the Newtonian linear relationship between the stress and the deformation rate with an additional factor of $1 + c[\eta]$, while for the $\tau^{22}$ transverse normal stress the boundary values at inflow and along the solid boundaries were simply zero, once again as in the Newtonian case. At this point a remark concerning the interpretation of the Cartesian stress components in the mid-section of the domain, where the flow is

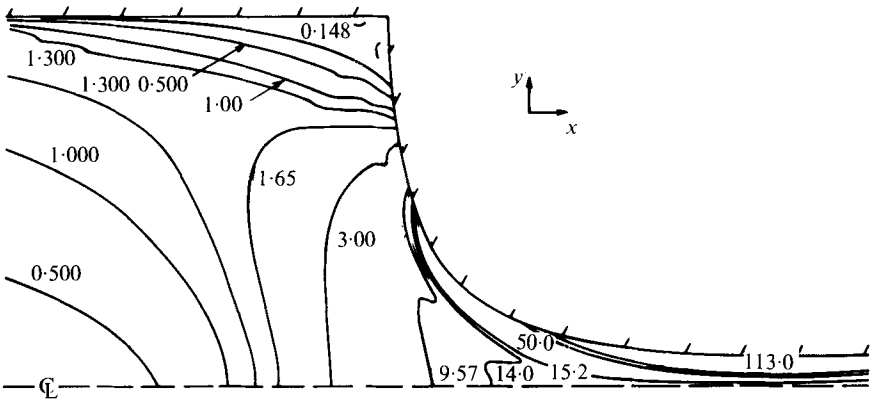


FIGURE 12. Contours of the strain rate in principal axes.

not parallel to the co-ordinate system, is in order. The $\tau^{12}$ shear stress, for example (note that analogous statements can be made concerning the Cartesian components of the normal stresses), is the shearing stress set up by a shearing motion in which parallel layers of fluid, which in the Cartesian system means parallel in the $x$ direction for $\tau^{12}$, move relative to one another. In the mid-section of the domain, however, the only appropriate co-ordinate system, i.e. one in which the shear stress is indeed a tangential force on a fluid element, would be one which is parallel and perpendicular to the streamlines. For this reason it is difficult to make any concise statements concerning the behaviour of the shear stress (or normal stress) in this region of the flow domain. Returning now to a discussion of the stresses, one sees that since the shear stress and transverse normal stress have essentially Newtonian characteristics throughout the flow the distinctive features of the non-Newtonian flow must be contained in the $\tau^{11}$ normal-stress distribution. These non-Newtonian $\tau^{11}$ normal-stress contours are plotted in figure 11 (*a*) and, for comparison, the Newtonian streamwise normal stress is shown in figure 11 (*b*) (recalling that $\tau^{22} = -\tau^{11}$ for a Newtonian fluid, one sees that the non-Newtonian $\tau^{22}$ normal-stress contours (figure 10) are indeed similar to their Newtonian counterparts in figure 11*b*). As can be seen, the magnitude of the stress levels has effectively doubled in most of the domain (not affected by molecular stretching) but, more important, the qualitative behaviour in the contraction region has changed substantially. This qualitative change can be explained if one considers the principal axes of the strain rate in the domain. The eigenvalues of the strain-rate matrix are given by

$$\lambda^{(1)} = -\lambda^{(2)} = [(S^{11})^2 + (S^{12})^2]^{\frac{1}{2}} \tag{4.1}$$

and the contours of these strain rates (in principal axes) are given in figure 12. The important feature of this plot is the nature of the contours in the contraction region. Comparison of the qualitative features of the eigenvalue contours and the non-Newtonian $\tau^{11}$ normal-stress contours indicates a coupling of the two variables. What has happened is that the molecules have aligned themselves with the principal axes, the deviation from the axes being a function of vorticity. Hence the characteristics of the non-Newtonian streamwise normal stress, i.e. the molecular component, are now similar to the characteristics of the strain-rate eigenvalues (the degree of similarity being a function of molecular alignment). Finally, note that in figure 11 (*a*) the

negative non-Newtonian $\tau^{11}$ stress levels have moved upstream relative to their Newtonian counterparts. This means that the extensional forces are increasing in the lower contraction region and, from further computational tests, are a function of the elasticity of the fluid. With a knowledge of the eigenvalues of the strain-rate matrix one can also determine whether the flow under investigation is a strong or a weak flow (Tanner 1976). Tanner points out that the flow is weak, i.e. molecular extension is small, if $\det[u_{i,j}\lambda_1 - \frac{1}{2}\delta_{ij}] < 0$, or following Lodge (1964) it is weak if simply $S_{11}\lambda_1 < \frac{1}{2}$. In the contraction region the above criteria are both satisfied, indicating a relatively weak flow and a small first normal-stress difference (Tanner & Stehrenberger 1971). This is a consequence of the small value for $\lambda_1$ needed for stable computations. Finally, the results of Tanner (1976) give a Weissenberg number $N_{wi}$ in this contraction region of $0{\cdot}24[\exp(2S^{11}\lambda_1) + 2\exp(-S^{11}\lambda_1 - 3)]^{\frac{1}{2}}$.

## 5. Concluding remarks

The investigation described here was an attempt to model numerically the full set of equations describing the steady flow of a non-Newtonian fluid through a complex geometry. If one is to understand fully the behaviour of macromolecules in a turbulent flow it is, of course, necessary to choose an appropriate constitutive equation as well as to model the turbulence itself. The full turbulent problem would require additional equations or models for the Reynolds stresses, and such a problem would naturally be limited by present computer capabilities. Our approach here was to experiment in a laminar flow with a numerical solution of the full set of equations governing the motion, including a rather complex constitutive equation. Such a flow with a varying vorticity field could give information on molecular behaviour which might occur in a turbulent flow, where the vorticity and strain-rate fields are randomly distributed. It was found that the character of this system of equations causes numerical problems which must be solved before extensive stretching of the molecules can be observed. For industrial applications in complex geometries, problems arise at irregular boundaries, forcing co-ordinate transformations for finite-difference methods or inversion of large-order matrices for finite-element methods. It appears that in the next step in the full numerical modelling of these equations a more efficient numerical technique is needed and, in addition, a more sophisticated constitutive equation could be used to model better the molecular extension. Nevertheless, our attempt here can act as a basis for future work in the area of polymer flows since a complete picture of the behaviour of the flow can be achieved only through the solution of a full set of equations and not just through a specification of a flow field and observation of the response of the fluid.

This work was supported in part by the U.S. Naval Sea Systems Command, through the Fluid Engineering Unit of the Applied Research Laboratory, and in part by the U.S. Office of Naval Research, Fluid Dynamics Branch; it formed part of the Ph.D. thesis of T. B. G. (Gatski 1976).

## REFERENCES


BLACK, J. R. & DENN, M. M. 1975 *J. Non-Newtonian Fluid Mech.* **1**, 83.

BLACK, J. R., DENN, M. M. & HSIAO, G. C. 1975 In *Theoretical Rheology* (ed. J. F. Hutton, J. R. A. Pearson and K. Walters), p. 3. Barking, England: Applied Science Publ.

DUDA, J. L. & VRENTAS, J. S. 1973 *Trans. Soc. Rheol.* **17**, 89.

GATSKI, T. B. 1976 The numerical solution of the steady flow of Newtonian and non-Newtonian fluids through a contraction. Ph.D. thesis, Pennsylvania State University, University Park.

GATSKI, T. B. 1978 Steady flow of a non-Newtonian fluid through a contraction. *J. Comp. Phys.* (to appear).

GIESEKUS, H. 1962 *Rheol. Acta* **2**, 50.

GIESEKUS, H. 1966 *Rheol. Acta* **5**, 29.

HUILGOL, R. R. 1975 *Rheol. Acta* **14**, 48.

LODGE, A. S. 1964 *Elastic Liquids*. Academic Press.

LUMLEY, J. L. 1969 *Ann. Rev. Fluid Mech.* **1**, 367.

LUMLEY, J. L. 1971 *Phys. Fluids* **14**, 2282.

LUMLEY, J. L. 1972*a* *Symposia Mathematica* vol. 9, p. 315. Academic Press.

LUMLEY, J. L. 1972*b* *Phys. Fluids* **15**, 217.

METZNER, A. B., UEBLER, E. A. & CHUN MAN FONG, C. F. 1969 *A.I.Ch.E. J.* **15**, 750.

OLDROYD, J. G. 1950 *Proc. Roy. Soc.* A **200**, 523.

PETERLIN, A. 1966 *J. Pure Appl. Chem.* **12**, 563.

PETERLIN, A. 1970 *Nature* **227**, 598.

ROACHE, P. J. 1972 *Computational Fluid Dynamics*. Albuquerque: Hermosa.

TANNER, R. I. 1975*a* *Trans. Soc. Rheol.* **19**, 557.

TANNER, R. I. 1975*b* *Trans. Soc. Rheol.* **19**, 37.

TANNER, R. I. 1976 *A.I.Ch.E. J.* **22**, 910.

TANNER, R. I. & STEHRENBERGER, W. 1971 *J. Chem. Phys.* **55**, 1958.

TOMS, B. A. 1948 *Proc. 1st Int. Cong. Rheol.* vol. 2, p. 135. North Holland.

TOWNSEND, P. 1973 *Rheol. Acta* **12**, 13.

WATERS, N. D. & KING, M. J. 1971 *J. Phys.* D, *J. Appl. Phys.* **4**, 204.